J. Indian Chem. Soc.,
Vol. 97, January 2020, pp. 75-84

Analytical methods for characterization of the mineralogical constituents of the urinary stones and influence of various factors for its reoccurrence

Ridhdhi laiya[a,b], Pragnya A. Bhatt[a], Anjani Bhatt[a] and Parimal Paul*[a,b]

[a]Analytical and Environmental Science Division & Centralized Instrument Facility,
CSIR-Central Salt and Marine Chemicals Research Institute, G. B. Marg, Bhavnagar-364 002, Gujarat, India

[b]P. D. Patel Institute of Applied Sciences, Charotar University of Science and Technology, Changa-388 421, Gujarat, India

E-mail: ppaul@csmcri.res.in

Manuscript received online 25 November 2019, accepted 26 December 2019

Urinary stone disease is common worldwide but systematic study for characterization of its constituents, particularly for reoccurred stones, and its correlation with the patients' dietary habit, metabolic disorder and other regional factors has not been much explored. Some of the areas, frequent recurrence of stones is common and therefore, we have undertaken analysis of the constituents of recurred stones and how its composition differs. For this purpose, 13 stones from five patients have been collected and analysed on the basis of powder XRD, FT-IR, TGA, SEM and EDX analysis. Powder XRD analysis suggests calcium oxalate monohydrate is the primary constituent of all stones, in addition to that a few of them also exhibit presence of calcium oxalate dihydrate and dolomite. IR study supported the composition suggested by XRD. TGA analysis exhibited loss of H_2O, CO and CO_2 at different temperatures and the mass loss is in agreement with the calculated values. SEM images exhibited morphology of the stones and EDX analysis confirmed the presence of calcium and other elements present in the stones. From powder XRD analysis, unit cell parameters and strain factor in the unit cell are calculated. The result obtained is discussed considering factors such as metabolic conditions, stone inhibitors, promoters, proteins etc.

Keywords: Urinary stone analysis, reoccurred stones, powder-XRD, SEM analysis, Whewellite and Weddellite.

Introduction

Human being has been suffering from the urinary stone related diseases since long, it causes substantial pain and occasional renal failure[1,2]. Urinary stones are hard solid, mostly irregular shape and found at three sites of the urinary tract, viz. kidney, ureter and bladder[3]. Though a considerable amount of research has been carried out to ascertain the cause of urinary stone formation, however, the mechanism of its formation is not yet fully understood[4–6]. There are number of factors, such as metabolic disorder, dietary habit, fluid intake, water quality, climate, urinary tract infection, occupation, stress etc. are probable causes of stone formation[7,8]. To study the mechanistic aspects of stone formation, it is essential to know the constituents of urinary stones and how the composition changes with the change of different factors. Therefore, it is essential to analyse the constituents of urinary stones and to correlate it with the factors, which influence its formation, as mentioned above. At present, there are no proven preventive measures to avoid urinary stone formation and once it is formed, it has to be removed either by surgery or through urinary track by applying proper medication, if it is diagnosed at the early stage. Once the stone is removed from the body, its constituents can be analysed using various analytical techniques[8–18]. Interestingly, the patient may not get rid of stone formation after its removal for the first time, recurrence, even for a number of times, is common[5,19–21]. It is therefore, necessary to characterize the stones recurred and how it differs from the one formed first.

Finlayson reviewed worldwide geographic surveys and documented the nationwide high incidence/low incidence areas[22]. North India comes under high incidence zone[23,24]. A number of researchers have made a further survey of some specific zones for a specific period and tried to understand the specificity of the urinary stone for the respective zone[24–28]. Saurashtra region of the Gujarat state, India, is one of the most urinary stone disease prone area. However, no sys-

tematic study on urinary stone formation and analysis of its constituents of this region has been carried out.

We have undertaken this study to find out the constituents of the reoccurred urinary stones using sophisticated analytical instruments and to correlate the composition with different factors, which influence stone formation. One of the objectives is to establish analytical methods for characterization of urinary calculi with reliability and accuracy. The other objectives are to investigate the difference in constituents, morphology and crystal parameters of the samples obtained from the same patient at different intervals of time due to recurrence. All this information is expected to enrich data base/literature, analysis of which may enlighten mechanistic aspects of stone formation and also about factors, which influence crystal formation and its morphology. Herein we report the characterization of urinary stones obtained from five patients of a city (Bhavnagar) of the west zone of India. These patients are in the age of 35 to 55 years, male and female and stones were recurred two to four times in the time span of two to five years. These stones were removed from the patient by surgery and the authors have received these samples either from Surgeon or from family members of the patient and used exclusively for this study. These samples were characterised on the basis of the PXRD, FT-IR, TGA, SEM and EDX analysis and the results obtained has been discussed in light of mechanistic aspects of stone formation, morphology and different crystal parameters and the factors, which influence stone formation.

Experimental

The samples of urinary stones were collected from Urologist and also from the patients, all of them belong to Bhavnagar city (Gujarat, India) and these stones were used exclusively for this study. These samples were dried for a week and grounded properly to collect various analytical data. Powder X-ray diffraction measurements have been performed using Philips X'Pert MPD Powder X-Ray Diffractometer. Measurements have been done from 5 to 80° 2θ range with the step size of 0.02°/s using CuKα radiation, operating at 40 KV and 30 mA. Constituents present in the stones have been identified by comparing the measured diffractograms with JC_PDF (joint committee for powder X-ray diffraction file), ICDD (international crystallographic diffraction data) database. Crystallite size and strain have been determined using the Scherrer's formula[29]. Unit cell has been determined using literature method for respective stones[30,31]. Percentage of crystallinity of the present phase has been determined using HighScore Plus software with the help of PXRD data. Quantification of urinary stones has been done using Rietveld refinement technique[32]. Infrared (IR) spectra were recorded on Perkin-Elmer Spectrum-GX FT-IR instrument using KBr pallet. Thermogravimetric analysis has been performed on a Mettler Toledo TGA instrument, model: SDTA851e, with a heating rate of 1°C/min, under the nitrogen atmosphere. SEM images were recorded on JSM-7100F Field Emission Scanning Electron Microscope (FESEM) with 15 kV LED operation voltage. The images were recorded at 60 to 43,000 magnification range. EDX analysis was done by pointing the probe to crystals under study and wave patterns were analysed. Optical images of the samples were recorded on an Olympus, model BX 16 microscope.

Results and discussion

Details about patients and urinary stones collected for this study:

Total 13 urinary stones were collected from five patients at different time intervals and for every patient, apart from the first stone, there are different number of recurred stones. Details about the patients, such as age, sex, food habit and stone removal procedure are summarized in Table 1 with sample codes. Optical images of four of the samples, including recurred stones, from two patients are shown in Fig. 1. The first one, KSARB-1, was a ureter stone and was surgically removed, whereas the second one, KSARB-2, was spontaneously excreted kidney stone and it was excreted just one month after the surgical removal of first stone. KSARB-3 was also a ureter stone and was surgically removed. Third and fourth stones were large (LBS) and small (SBS) bladder stone from the same patient. The full grains and their cross section views were examined and the images are displayed in Fig. 1, it may be noted that the outer surface and cross-sectional views are significantly different.

Powder X-ray diffraction study:

Powder X-ray diffraction (PXRD) of all the 13 samples were recorded and diffraction patterns of the four recurred samples of the first patient (KSHIM 1-4), three recurred stones of the second patient (KSARB 1-3) and two recurred samples

Table 1. Details of sample collected and patients' information

Patient code	Sex	Age	Food	No. of stone	Sample code	Removal procedures
KSHIM	M	55	Veg*	4	KSHIM-1	Surgically removed (Lithotripsy)
					KSHIM-2	Spontaneously excreted
					KSHIM-3	Spontaneously excreted
					KSHIM-4	Spontaneously excreted
KSARB	M	55	Veg	3	KSARB-1	Surgically removed (Ureteroscopy)
					KSARB-2	Spontaneously excreted
					KSARB-3	Surgically removed
HITESH	M	40	Veg	2	KSHITESH-1	Surgically removed (Lithotripsy)
					KSHITESH-2	Spontaneously excreted
TRIVEDI	F	55	Veg	2	KST-1	Surgically removed (Lithotripsy)
					KST-2	Surgically removed
BS	M	55	Veg	2	LBS	Auto excretion
					SBS	Auto excretion

Veg* = Vegetarian.

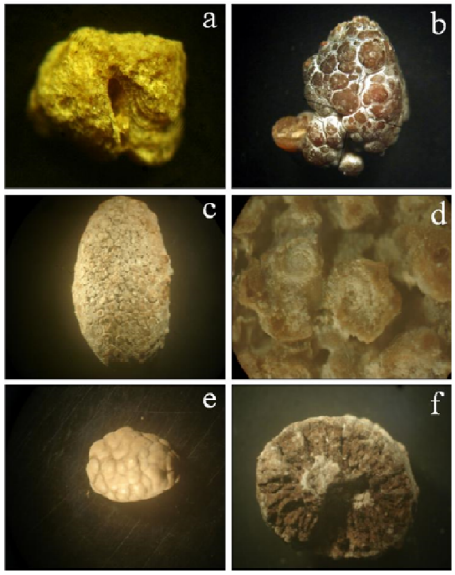

Fig. 1. Optical microscopic images of urinary stones: (a) stone removed from ureter KSARB-1, (b) spontaneously excreted stone KSARB-2, (c) bladder stone LBS, (d) cross sectional view of LBS, (e) small bladder stone SBS and (f) cross sectional view of SBS.

of the third patient (KSHITESH 1-2) are displayed in Fig. 2. Two samples of the fourth patient (KST 1-2) and two samples of the fifth patient (LBS and SBS) are shown in Fig. 3. Phase identification of the diffractograms was carried out on the basis of JC-PDF number, % crystallinity, unit cell parameters, size of the unit cell in Å and strain in the percentage of all the samples were calculated and all the results are summarized in Table 2. It may be noted in Table 2 that the constituent of all the four stones of the first patient is same and it is Whewellite (calcium oxalate monohydrate), the unit cell parameters are similar, however the size of the unit cells is significantly different, which suggests that the packing pattern of the molecules in the unit cell is quite different. For the second patient, there are three samples (KSARB 1-3), two of these samples (KSARB-1 and 2) contain pure calcium oxalate monohydrate, however, KSARB-2 contains mixed phases, calcium oxalate monohydrate with dolomite, which is not common. The unit cell parameters of KSARB-1 and 3 are similar to that of the first patient; however, it is significantly different for KSARB-2, as it has accommodated the dolomite phase, the unit cell parameters and unit volume of which is quite different from other two samples. For the third patient, the constituent, unit cell parameters and size of the unit cell are similar to that of KSARB-1 and KSARB-3 of patient 1, respectively. For the fourth patient (Fig. 3), the first sample (KST-1), contains pure Whewellite phase but the second sample contains mixed phases, Whewellite and Iron (minor), which is unusual in the case of a human kidney stone. The unit cell parameters and size of these two samples are quite different from other samples reported here. The samples SBS and LBS are two bladder stones obtained from the same patient (fourth). Both of these two samples contain mixed phases, calcium oxalate monohydrate (COM) and calcium oxalate dihydrate (COD) COM phase and 40.9% of COD

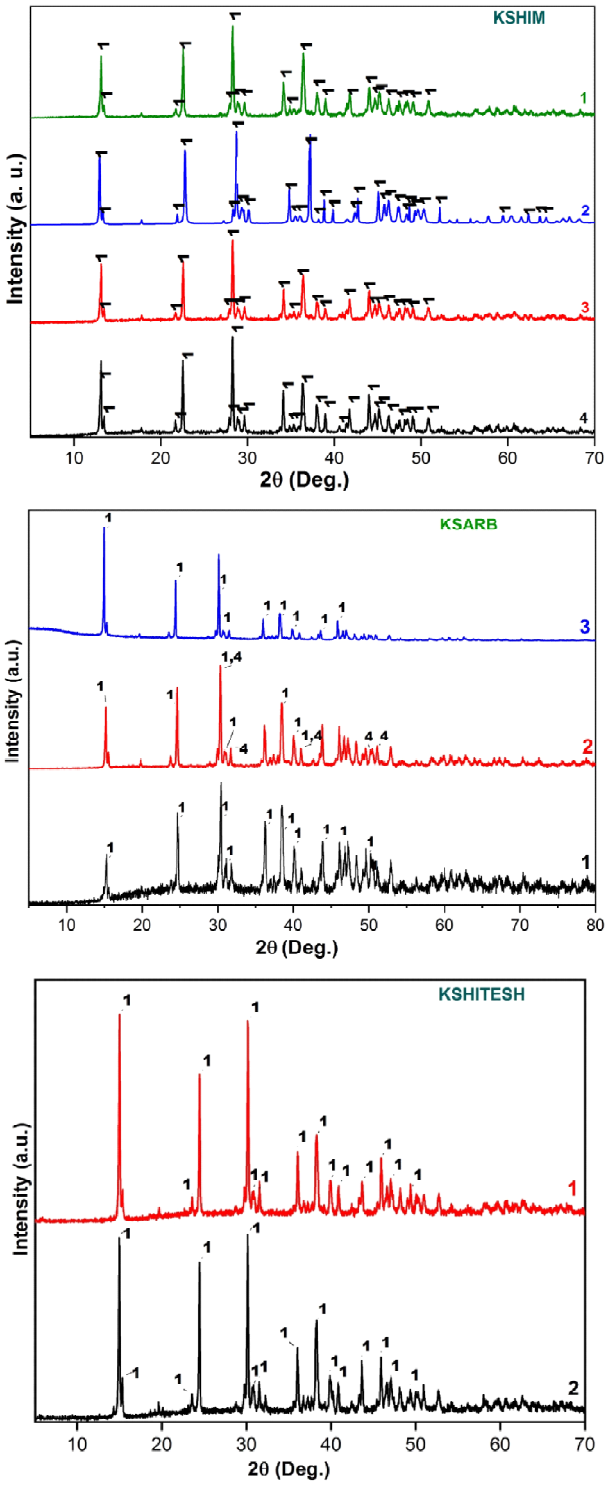

Fig. 2. Diffractograms of urinary stones from different patients: KSHIM 1-4, four recurred samples of the first patient, KSARB 1-3, three recurred stones from the second patient and KSHITESH 1-2, two recurred samples of the third patient are shown. Peaks designated with '1', '2' and '4' are due to Whewellite, Weddellite and Dolomite phases, respectively.

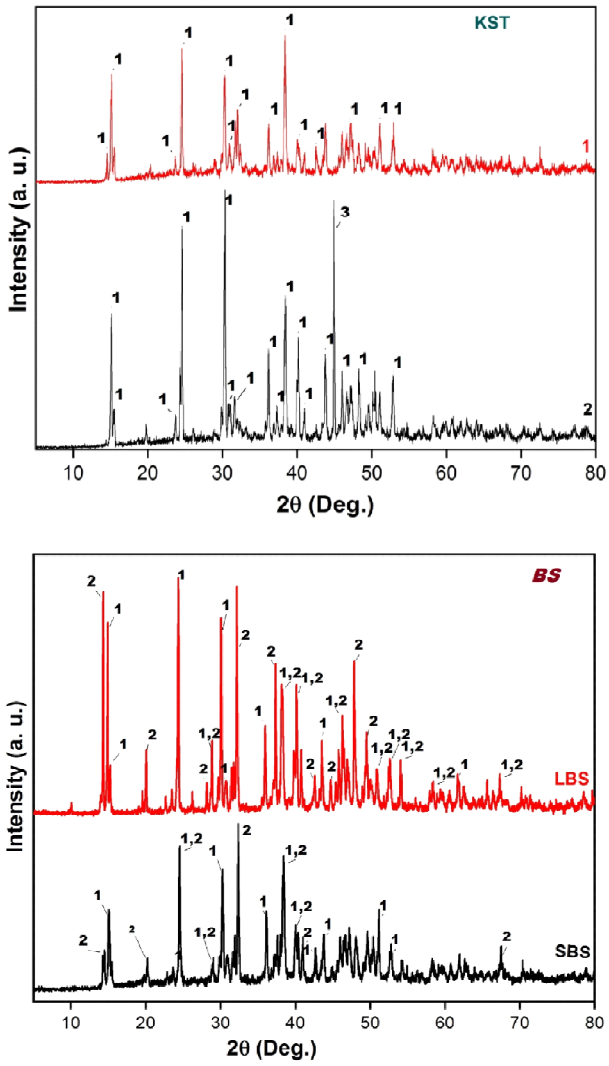

Fig. 3. Diffractograms of urinary stones from different patients: KST 1-2, two recurred samples of the fourth patient and SB (LBS and SBS), two samples of the fifth patient are shown. Peaks designated with '1', '2' and '3' are due to Whewellite, Weddellite and Iron phases, respectively.

phase. A larger proportion of COM phase in SBS stone may be attributed to probable conversion of COD phase into COM phase because COD phase is less stable compared to COM phase[1,33]. SBS being excreted at the later time, the reason therefore justified. The powder XRD data therefore conclusively determined the constituents of the urinary stones and also revealed that the constituents of the recurred stones of the same patient are not necessarily the same, it may differ though environment, food habit and other physiological conditions are expected to be similar.

Table 2. Phase identification and unit cell parameters of stones from PXRD data

Sample code	JC-PDF number	Present phase	%, Crystallinity	Unit cell parameters a, b, c in Å and α, β, γ in°	Size (nm)	Strain (%)
KSHIM-1	00-020-0231	COM*	97.96	a=9.97, b=7.29, c=6.29, β=107	286.2	0.252
KSHIM-2	00-020-0231	COM	80.59	a=9.983, b=7.306, c=6.2981, β=107.025	148.4	0.371
KSHIM-3	00-020-0231	COM	90.10	a=9.986, b=7.304, c=6.275, β=107.019	119.6	0.424
KSHIM-4	00-020-0231	COM	89.55	a=10.11, b=7.29, c=6.29, β=109.45	81.8	0.545
KSARB-1	00-020-0231	COM	81.95	a=9.9881, b=7.235, c=6.680, β=106.97	119.6	0.419
KSARB-2	00-020-0231	COM	93.96	a=8.84, b=8.00, c=6.20, β=106.76	167.0	0.342
	00-011-0078	Dolomite	–	a=4.81, b=4.81, c=16.02, γ=120	36.6	0.475
KSARB-3	00-016-0379	COM	97.95	a=9.96, b=7.30, c=6.27, β=106.82	–	–
KSHITESH-1	00-020-0231	COM	86.49	a=9.976, b=7.296, c=6.292, β=107.016	286.2	0.254
KSHITESH-2	00-020-0231	COM	91.19	a=9.978, b=7.294, c=6.292, β=107.055	119.6	0.426
KST-1	00-020-0231	COM	88.15	a=13.59, b=13.67, c=6.46, β=91.755	75.6	0.573
KST-2	00-020-0231	COM	85.75	a=7.53, b=9.97, c=5.93, β=106.70	170.5	0.340
	00-003-1050	Iron	–	a=b=c=2.85, α=β=γ=90	>Max	0.041
SBS	00-020-0231 (73%)	COM	82.83	a=10.041, b=7.341, c=6.31, β=107.031	75.6	0.573
	00-017-0541 (27%)	COD*	–	a=12.365, b=12.365, c=7.3463, α=β=γ=90	35.7	1.04
LBS	00-020-0231 (59.1%)	COM	100.36	a=9.980, b=7.296, c=6.294, β=107.022	286.2	0.254
	00-017-0541 (40.9%)	COD	–	a=12.365, b=12.365, c=7.3463, α=β=γ=90	286.0	0.265

*COM – Calcium oxalate monohydrate, COD – Calcium Oxalate dihydrate.

FT-IR study:

IR spectra of all the samples were recorded as a complementary study to confirm the presence of compounds/functional groups revealed by the powder X-Ray diffraction study. The IR spectra of 11 samples of four patients are displayed in Figs. 4 and 5. It may be noted that FT-IR spectra of all the four urinary stones of the first patient (Fig. 4, KSHIM 1-4) are similar and they consist of the characteristic bands of Whewellite phase[8]. The bands in the range 3500–3200 cm^{-1} are due to the symmetric and asymmetric stretch of the water molecule, whereas the strong band around 1620 cm^{-1} and the weak band at 661 cm^{-1} are due to bending and wagging modes of the water molecule[34,35]. The bands at 1665, 1316, 780 and 518 cm^{-1} are due to ν_a(C=O), ν_s(C=O), δ(O-C=O) and ν(Ca-O) frequencies of the oxalate moiety[35,36]. The IR spectra of the three stones of second patient (KSARB 1-3) exhibit characteristic bands of calcium oxalate monohydrate, as described above. In addition to that KSARB-2 exhibited three strong bands in the mid-infrared region, which are due to CO_3^{2-} anion of the dolomite phase[37]. The bands at 1426, 874 and 713 cm^{-1} are assigned to the fundamental vibrations: ν_3 asymmetric stretching, ν_2 out-of-plane bending and ν_4 in-plane bending, respectively. The two IR spectra of the third patient (KSHITESH-1 and KSHITESH-2) exhibit bands correspond to the Whewellite phase, as seen for the first patient. The IR spectra of the two stones from the fourth patient (Fig. 5, KST-1 and KST-2) also exhibited bands correspond to the Whewellite phase. The spectra of two bladder stones from the same patient, the large (LBS) and the small bladder stone (SBS) showed the presence of characteristic bands of calcium oxalate monohydrate phase and in addition to that they also exhibited multiple bands in the region 3500–3300 cm^{-1}, which suggests the presence of calcium oxalate dihydrate[38]. The other bands at 1318 and 780 cm^{-1} are due to O-C-O and C-C stretching frequency of Weddellite phase, respectively.

Thermogravimetric analysis (TGA):

Powder XRD and IR analysis of the urinary samples sug-

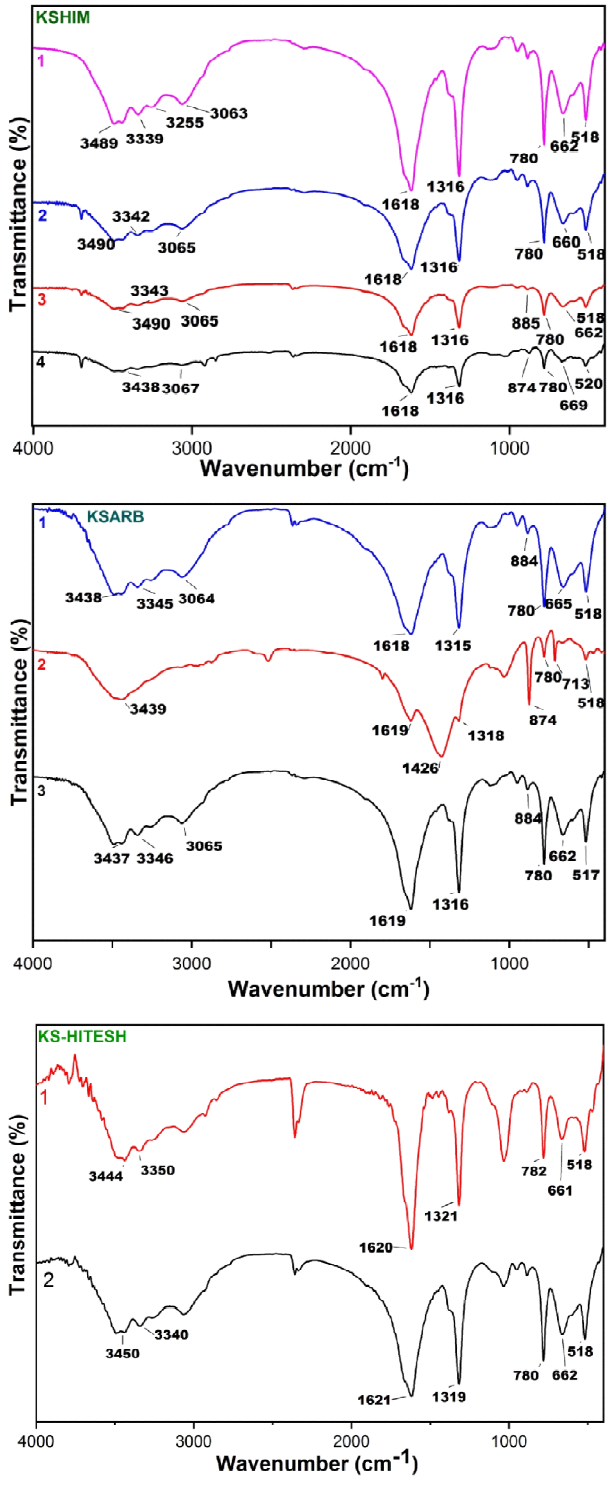

Fig. 4. The IR spectra of the urinary stones from first (KSHIM), second (KSARB) and third (KSHITESH) patients.

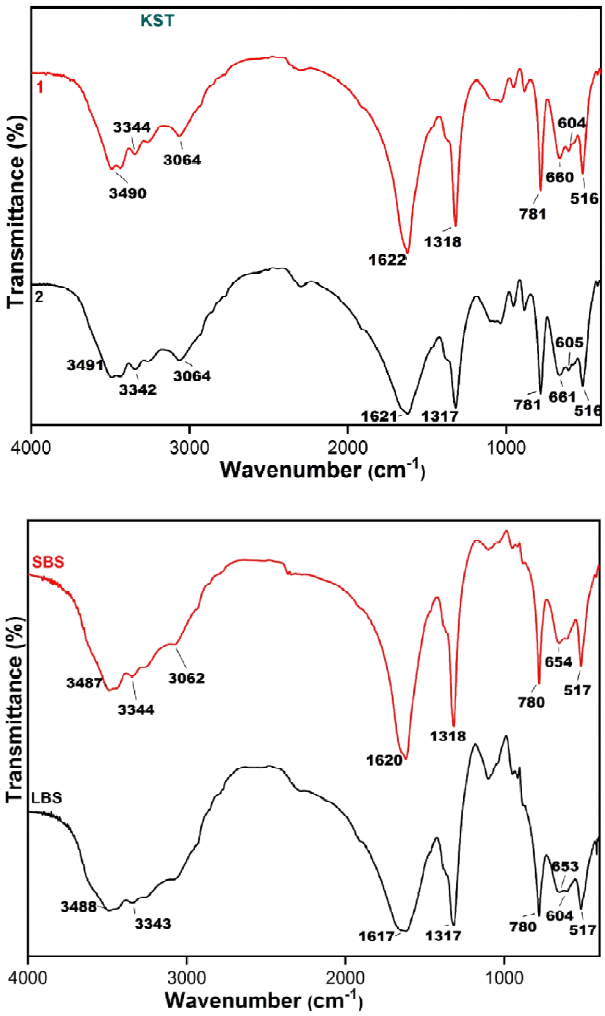

Fig. 5. The IR spectra of the urinary stones from fourth (KST) and fifth (SBS) patients.

gest calcium oxalate monohydrate (Whewellite) is the main constituent of these stones, in few cases calcium oxalate dihydrate is also noted. Therefore, it was interesting to study thermogravimetric analysis, as it is expected to provide information about the loss of water molecule upon heating the sample and also the loss of CO and CO_2 formed by thermal decomposition of the oxalate anion, which is the constituent of the stones. This study not only provides information about the mass/molecule loss as a function of temperature increase but also about the purity of the phases. With this aim, six of the stones were chosen as representative samples for this TGA analysis. The thermograms of the four samples (KSARB-1 and 2, LBS and SBS) are shown in Fig. 6 and the data for all samples with interpretation is given in Table 3. From the figure it is clear that for all of the four samples, weight loss has taken place in three steps, calculation of mass loss re-

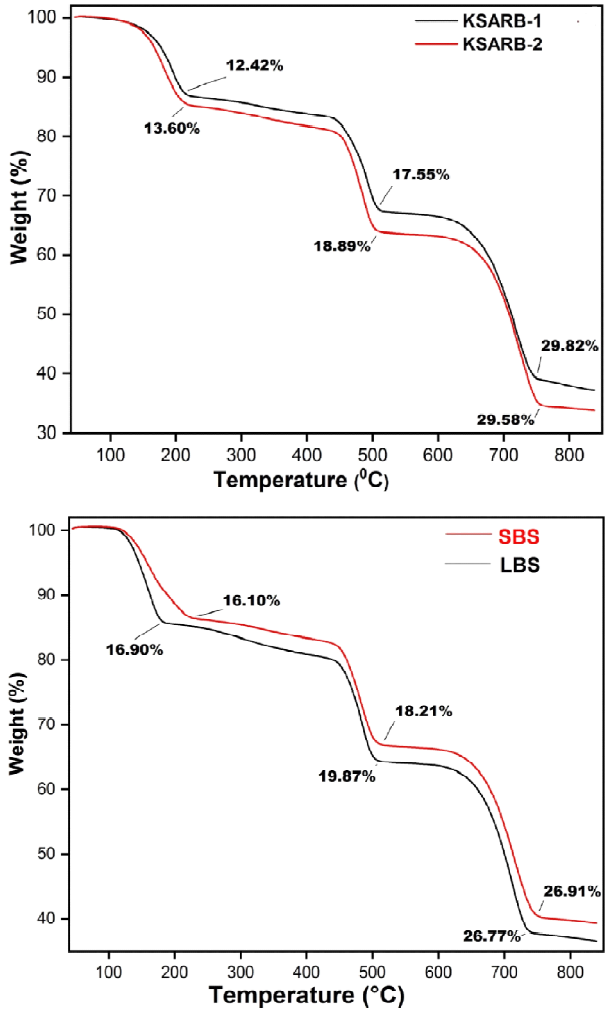

Fig. 6. Thermograms of the urinary stones KSARB-1, KSARB-2, LBS and SBS.

vealed that the mass loss of the first step between 100 and 200°C is due to loss of water molecule(s), the second and third steps of mass loss between 420 to 520°C is due to loss of CO and between 600 and 700°C is due to loss of CO_2. With increasing temperature, calcium oxalate monohydrate converted to calcium oxalate losing the water molecule; calcium oxalate on further heating converted to calcium carbonate losing CO, which on further heating formed calcium oxide and CO_2. The calculated loss of mass in percentage for all three steps for the samples KSARB-1 and 2 are in excellent agreement with the experimental values (Table 3). For the samples LSB and SBS, the loss of mass has been calculated taking into consideration of the presence of mixed phases with 73% of COM and 27% of COD for SBS and 59.1% of COM and 40.9% of COD for LBS and the results are in excellent agreement with the experimental values. The TGA analysis, therefore further confirmed the finding revealed by powder-XRD and IR analysis.

Scanning electron microscopic study (SEM):

To investigate the morphology of the constituent(s) of the stones, particularly for the recurred samples, and also for elemental analysis, scanning electron microscopic images (SEM) of some selected samples were recorded and energy dispersive X-ray (EDX) analysis of the same samples was also carried out. Sample preparation is a crucial step for recording SEM images, in this case, samples of urinary calculi were dried, finely grounded and then the mass was sonicated in acetone, the fine suspended particles were then dispersed on brass studs. To make the studs conductive, it was coated with 15 nm thickness of gold using a sputter coater and then the images were recorded. The SEM images of KSARB-2, KSARB-3, KST-1, KST-2 and SBS were shown in Fig. 7. It may be noted that the morphology of the samples are distinctly different, though constituent is same. Fig. 7a and 7b exhibit the SEM image of KSARB-2 and 3, which contains calcium oxalate monohydrate and the crystals appeared in the stacking of deposited components with layered morphology. On the other hand, the SEM images of KST-1 and KST-2, shown in Fig. 7c and 7d, respectively also contain calcium oxalate monohydrate but the morphology is distinctly different from each other and also different from that of KSARB-3. Fig. 7c showed no systematic shape, but the edge of the crystal showed layers of deposited components with smooth appearance whereas for the recurrence sample (KST-2, Fig. 7d), the morphology appeared as an aggregation of the components in the irregular shape. The morphology of the SEM image of the SBS (Fig. 7e and 7f), which contains calcium oxalate monohydrate (COM) and calcium oxalate dihydrate (COD), are close to that of KST-2, which appeared as an aggregation of crystals of irregular shape.

EDX analysis:

EDX analysis of the SEM images was carried out to find out the element present. The EDX analysis of KST-1 and KST-2 are shown in Fig. 8, which clearly exhibit the presence of calcium (17.62, 18.74%), oxygen (54.62, 58.20%) and carbon (27.76, 23.07%), confirming further the observation noted in powder-XRD.

Table 3. Thermogravimetric analysis of urinary stones

Sample code	Decomposition temperature-range	Calculated mass loss (%)	Experimental mass loss (%)	Deviation in mass loss (+/–) (%)	Decomposed phase
KSARB-1	120–200	12.30	12.42	0.12	H_2O
	420–520	19.17	17.55	1.62	CO
	600–700	30.12	29.82	0.3	CO_2
KSARB-2	120–200	12.30	13.60	1.3	H_2O
	420–500	19.17	18.89	0.28	CO
	600–700	30.12	29.58	0.54	CO_2
KSHITESH-1	100–210	12.30	13.28	0.98	H_2O
	400–520	19.17	25.32	6.15	CO
	540–720	30.12	43.62	13.5	CO_2
KSHITESH-2	120–230	12.30	11.88	0.42	H_2O
	410–550	19.17	22.03	2.86	CO
	590–740	30.12	30.24	0.12	CO_2
LBS	120–200	16.52	16.90	0.38	H_2O
	420–520	19.17	19.88	0.71	CO
	600–700	30.12	26.78	3.34	CO_2
SBS	120–200	15.15	16.10	0.86	H_2O
	420–500	19.17	18.21	0.96	CO
	600–700	30.12	26.91	3.21	CO_2

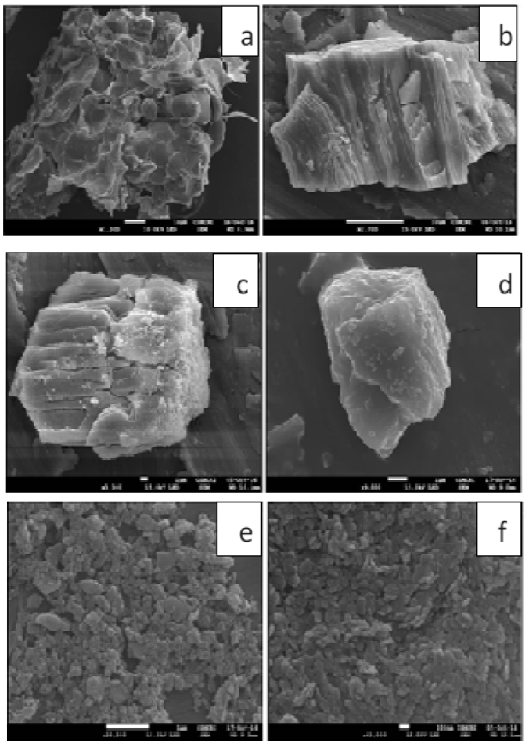

Fig. 7. SEM images of the urinary calculi of KSARB-2 (a), KSARB-3 (b), KST-1 (c), KST-2 (d), SBS (e) Whewellite and (f) Weddellite phases.

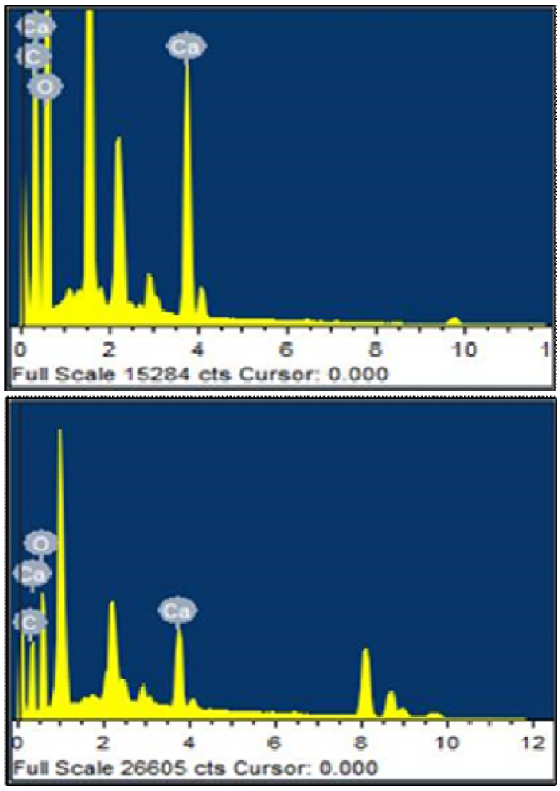

Fig. 8. EDX analysis of Whewellite phase of the stones (a) KST-1 and (b) KST-2.

This study therefore revealed that calcium oxalate monohydrate is the main constituents of the urinary stones, however the presence of other components such as dolomite and calcium oxalate dihydrate is also evident in few cases. For recurred stones, though the constituent is same as for the first stone for most of the cases, however their unit cell parameters, particularly the size and strain factor (in percentage) are significantly different (Table 2). SEM images also revealed a significant difference in morphology for the stones from the same patient, which is consistent to the observation of differences in unit cell parameters and it suggests that the packing and/or orientation of the constituent molecule(s) in the unit cell is different. The food habits (all are vegetarian), climate and physiological conditions under which crystals recurred are same for the same patient and similar for the patients reported here, therefore some factors, other than those just mentioned probably have an impact on crystal growing/packing in the unit cell. The unique metabolic condition over a period of time for a particular patient might have an influence on crystal growing/packing[39–41]. Changes in phase or morphology of stones over a period could also be due to the dynamic changes in urine composition over a period of time. The presence of COM and COD containing phases may be attributed to low urinary volumes; high rates of calcium, oxalate, excretion; and low citrate and magnesium excretion, all of which increase calcium oxalate super saturation. Once, its concentration exceeds its thermodynamic solubility product in water (KSP), crystallization can occur. In urine, crystal nuclei usually form on existing surfaces (heterogeneous nucleation). Heterogeneous nucleation together with crystal growth and aggregation result into urinary stone. The presence of inhibitors such as magnesium and citrate in urine inhibits crystal aggregation. Nephrocalcin and acidic glycoprotein of renal origin also inhibit calcium oxalate nucleation, growth and aggregation[42]. Tamm-Horsefall mucoprotein, the most abundant protein in urine inhibit aggregation[43], whereas uropontin inhibits crystal growth[44]. Patients exhibit frequent stone formation may not be having the presence of such inhibitors in their urine, instead they might be having the presence of promoters in their urine[45,46].

Conclusions

Constituents of 13 recurred urinary stones from five patients from western India has been determined on the basis of PXRD and FT-IR analysis. These stones were removed from the patients either by surgery or obtained from spontaneous excretion through urine. Analysis of these stones revealed that calcium oxalate monohydrate is the constituent of all these samples in pure form in most of the cases and in few cases dolomite/calcium oxalate dihydrate is found. TGA analysis exhibited loss of H_2O, CO and CO_2 at three well separated distinct temperatures and the mass loss in the thermogram matched well with the mass of the species lost. CO and CO_2 were generated by the thermal decomposition of the oxalate anion and the TGA analysis further confirmed the constituents of the stones revealed by PXRD and FT-IR analysis. SEM images suggest that the morphology of the stones is significantly different though the constituent is same, it is consistent to the finding of different unit cell parameters and strain percentage in unit cell from PXRD study. Therefore, for recurred stones of the same patient, the constituent(s), morphology, unit cell parameters, strain factor and packing of the molecule(s) in unit cell may differ depending on metabolic conditions, presence/absence/variation of stone inhibitors, promoters, protein etc.

Acknowledgements

We thank Dr. P. K. Ghosh (former Director of CSIR-CSMCRI) for encouragement and support during this work, Mr. Vinod Agarwal for recording IR spectra and Mr. Jayesh Chaudhari for recording SEM images and EDX analysis. We also thank Council of Scientific and Industrial Research (CSIR), New Delhi for generous support towards infrastructures and core competency development.

References

1. M. L. Giannossi and V. Summa, "An Introduction to the Study of Mineralogy", eds. Cumhur Aydinalp, Tech, Europe and China, 2012, Chap. 7, pp. 123-146.
2. U. C. Jayaraman and A. Gurusam, *IOSR J. Pharm.,* 2018, **8**, 30.
3. S. Bhattacharyya, G. Sharma, A. K. Mandal and S. K. Singh, *J. Postgrad. Med. Edu. & Res.,* 2014, **48**, 128.
4. V. K. Singh and P. K. Rai, *Biophys. Reviews,* 2014, **6**, 291.
5. P. Durgawale, A. Shariff, A. Hendre, S. Patil and A. Sontakke, *Biomed. Res.,* 2010, **21**, 305.
6. A. P. Evan, E. M. Worcester, F. L. Coe, J. Williams and J. E. Lingeman, *Urolithiasis,* 2015, **43**, 19.
7. V. Sodimbaku and L. Pujari, *Int. J. Pharm. Pharm. Sci.*, 2014, **6**, 23.
8. P. A. Bhatt and P. Paul, *J. Chem. Sci.*, 2008, **120**, 267.

9. L. V. Didenko, E. R. Tolordava, T. S. Perpanova, N. V. Shevlyagina, T. G. Borovaya, Y. M. Romanova, M. Cazzaniga, R. Curia, M. Milani, C. Savoia and F. Tatti, *J. Appl. Med. Sci.,* 2014, **3**, 19.
10. K. Proksova, K. Novotny, M. Galiova, T. Vaculovic, J. Kuta, M. Novackova and V. Kanicky, *CHEMICKE LISTY,* 2012, **106**, 229.
11. H. P. Lee, D. Leong and C. T. Heng, *Urol. Res*., 2012, **40**, 197.
12. V. Uvarov, I. Popov, M. Shapur, T. Abdin, O. N. Gofrit, D. Pode and M. Duvdevani, *Environ. Geochem. Health,* 2011, **33**, 613.
13. P. Chatterjee, S. Pramanik and A. K. Mukherjee, *J. Appl. Cryst.,* 2015, **48**, 1794.
14. A. K. Mukherjee, *J. Indian Inst. Sci.,* 2014, **94**, 35.
15. A. Primiano, S. Persichili, G. Gambaro, P. M. Ferraro, A. D'Addessi, A. Cocci, A. Schiattarella, C. Zuppi and J. Gervasoni, *Disease Markers*, 2014, **2014**, 1.
16. V. S. Joshi, S. R. Vasant, J. G. Bhatt and M. Joshi, *Indian J. BioChem. BioPhys.,* 2014, **51**, 237.
17. T. Jindal, S. Mandal, P. Sonar, M. R. Kamal, N. Ghosh and D. Karmakar, *Adv. Biomed. Res.,* 2014, **3**, 203.
18. M. S. YalçIna and M. Tekb, *J. Appl. Spectrosco.,* 2019, **85**, 1050.
19. A. Skolarikos, M. Straub, T. Knoll, K. Sarica, C. Seitz, A. Petř ík f,g and C. Türk h, *Eur. Urol.,* 2015, **67**, 750.
20. A. Oddsson, P. Sulem, H. Helgason, V. O. Edvardsson, G. Thorleifsson, G. Sveinbjörnsson, E. Haraldsdottir, G. I. Eyjolfsson, O. Sigurdardottir, I. Olafsson, G. Masson, H. Holm, D. F. Gudbjartsson, U. Thorsteinsdottir, O. S. Indridason, R. Palsson and K. Stefansson, *Nat. Commun.,* 2015, **6**, 1.
21. A. Meyers, N. Whalley and M. Martins, *Afr. J. Nephro.,* 1998, **2**, 12.
22. B. Finlayson, *Urol Clin. North Am.,* 1974, **1**, 181.
23. R. Ganesamoni, S. K. Singh, in: J. J. Talati, H. G. Tiselius, D. M. Albala, Z. Ye (eds), "Urolithiasis: basic, science and clinical practice", Springer, London, 2012, pp. 39-46.
24. M. S. Ansari, N. P. Gupta, A. K. Hemal, P. N. Dogra, A. Seth, M. Aron and T. P. Singh, *Int. J. Urol.,* 2005, **12**, 12.
25. P. J. Carson and D. R. Brewster, *J. Paediatr. Child Health,* 2003, **39**, 325.
26. A. Terai, Y. Okada, T. Ohkawa, O. Ogawa and O. Yoshida, *Int. J. Urol.,* 2000, **7**, 452.
27. V. Romero, H. Akpinar and D. G. Assimos, *Rev. Urol.,* 2010, **12**, e86.
28. W. Wang, J. Fan, G. Huang, J. Li, Xi. Zhu, Y. Tian and L. Su, *Sci. Rep.* 2017, **7**, article number 41630.
29. P. Scherrer, *Nachr. Ges. Wiss. Göttingen,* 1918, **2**, 96.
30. T. J. B. Holland and S. A. T Redfer, *Mineralogical Magazine*, 1997, **61**, 65.
31. J. W. Visser, *J. Appl. Cryst.,* 1969, **2**, 89.
32. T. C. Santini, *Inter. J. Mineral Processing*, 2015, **139**, 1.
33. C. Conti, L. Brambill, C. Colombo, D. Dellasega, G. D. Gatta, M. Realini and G. Zerbi, *Phys. Chem. Chem. Phys.,* 2010, **12**, 14560.
34. D. Bazin, C. Leroy, F. Tielens, C. Bonhomme, L. B. Coury, F. Damay, D. L. Denmat, J. Sadoine, J. Rode, V. Frochot, E. Letavernier, J. Philippe Haymann and M. Daudon, *Comptes Rendus Chimie*, 2016, **19**, 1492.
35. G. S. Popescu, I. Ionescu, R. Grecu and A. Preda, *Revista Românã de Medicinã de Laborator*, 2010, **18**, 67.
36. L. Estepa and M. Daudon, *Biospectroscopy,* 1997, **3**, 347.
37. O. S. Pokrovsky, J. A. Mielczarski, O. Barres and J. Schott, *Langmuir*, 2000, **16**, 2677.
38. R. L. Frost, J. Yang and Z. Ding, *Chin. Sci. Bull.,* 2003, **48**, 1844.
39. A. Skolarikos, M. Straub, T. Knoll, K. Sarica, C. Seitz, A. Petř ík and C. Türk, *Euro. Urol.,* 2015, **67**, 750.
40. H. Tiselius, M. Daudon, K. Thomas and C. Seitz, *Euro. Urol. Focus,* 2017, **3**, 62.
41. S. Ranabir, M. P. Baruah and K. R. Devi, *Ind. J. Endo. Meta*., 2012, **16**, 228.
42. Y. Nakagawa, M. Ahmed, S. L. Hall, S. Deganello and F. L. Coe, *J. Clin. Invest.,* 1987, **79**, 1782.
43. B. Hess, Y. Nakagawa, J. H. Parks and F. L. Coe, *Am. J. Physiol.,* 1991, **260**, F569.
44. H. Shiraga, W. Min, W. J. VanDusen, M. D. Clayman, D. Miner, C. H. Terrell, J. R. Sherbotie, J. W. Foreman, C. Przysiecki and E. G. Neilson, *Proc. Natl. Acad. Sci.,* 1992, **89**, 426.
45. M. Gupta, S. Bhayana and S. K. Sikka, *Inter. J. Res. Pharm. Chem.*, 2011, **1**, 793.
46. D. R. Basavaraj, C. S. Biyani, A. J. Browning and J. J. Cartledge, *eau-ebu update series,* 2007, **5**, 126.